Alexandria Engineering Journal (2014) **53**, 259–273

Alexandria University

Alexandria Engineering Journal

www.elsevier.com/locate/aej
www.sciencedirect.com

ORIGINAL ARTICLE

Performance, emission and combustion characteristics of a diesel engine using Carbon Nanotubes blended Jatropha Methyl Ester Emulsions

J. Sadhik Basha [a,*], **R.B. Anand** [b,1]

[a] *Department of Mechanical Engineering, King Khalid University, Abha, Kingdom of Saudi Arabia*
[b] *Department of Mechanical Engineering, National Institute of Technology, Tiruchirappalli 620 015, Tamil Nadu, India*

Received 26 July 2013; revised 13 August 2013; accepted 2 April 2014
Available online 29 April 2014

KEYWORDS

Jatropha Methyl Esters;
Emulsion;
Carbon Nanotubes;
Emissions;
Diesel engine

Abstract An experimental investigation was conducted in a single cylinder constant speed diesel engine to establish the effects of Carbon Nanotubes (CNT) with the Jatropha Methyl Esters (JME) emulsion fuel. The JME was produced from the Jatropha oil by transesterification process, and subsequently the JME emulsion fuel was prepared in the proportion of 93% of JME, 5% of water and 2% of surfactants (by volume) with a hydrophilic–lipophilic balance of 10. The Carbon Nanotubes are blended with the JME emulsion fuel in the various dosages systematically. The whole investigation was conducted in the diesel engine using the following fuels: neat JME, neat JME emulsion fuel and CNT blended JME emulsion fuels accordingly. The experimental results revealed an appreciable enhancement in the brake thermal efficiency for the CNT blended JME emulsion fuels compared to that of neat JME and neat JME emulsion fuel. At the full load, the brake thermal efficiency for the JME fuel observed was 24.80%, whereas it was 26.34% and 28.45% for the JME2S5W and JME2S5W100CNT fuels respectively. Further, due to the combined effects of micro-explosion and secondary atomization phenomena associated with the CNT blended JME emulsion fuels, the level of harmful pollutants in the exhaust gases (such as NO_x and smoke)

---

[*] Corresponding author. Tel.: +966 5943 26 226; fax: +966 72419113.
E-mail addresses: mailsadhik@gmail.com (J. Sadhik Basha), rbanand@nitt.edu (R.B. Anand).
[1] Tel.: +91 431 250 3409; fax: +91 431 250 0133.

Peer review under responsibility of Faculty of Engineering, Alexandria University.

Production and hosting by Elsevier

http://dx.doi.org/10.1016/j.aej.2014.04.001

was drastically reduced when compared to that of neat JME. At the full load, the magnitude of NO_x and smoke opacity for the neat JME was 1282 ppm and 69%, whereas it was 910 ppm and 49% for the JME2S5W100CNT fuel respectively.

Nomenclature

bmep	brake mean effective pressure, bar
bTDC	before Top Dead Center
CA	crank angle
CNT	Carbon Nanotube
CO	Carbon Monoxide
JME	Jatropha Methyl Esters
JME2S5W	93% Jatropha Methyl Esters + 2% surfactant + 5% water
JME2S5W25CNT	93% Jatropha Methyl Esters + 2% surfactant + 5% water + 25 ppm CNT
JME2S5W50CNT	93% Jatropha Methyl Esters + 2% surfactant + 5% water + 50 ppm CNT
JME2S5W100CNT	93% Jatropha Methyl Esters + 2% surfactant + 5% water + 100 ppm CNT
HC	Hydrocarbons, ppm
HLB	Hydrophilic–Lipophilic Balance

1. Introduction

In the context to the global energy scenario, the technical community is presently confronted with the twin crises of fossil fuels diminution and environmental degradation. The indiscriminate extraction and lavish consumption of fossil fuels have led to reduction in the underground derived carbon resources, and thus triggered the researchers to impart active research interest in non-petroleum, renewable and eco-friendly fuels. The world oil reserves are obviously limited and are expected to diminish for another few years owing to the enormous growth of world population, enhanced technical sophistication and exorbitant industrialization. The fossil fuel (particularly diesel) utilized by diesel engines has played a critical role in all the major sectors (such as transportation, power, industry, marine, agricultural) owing to their fuel economy, sturdiness, reliability and rigidity. But at the same time they emit hazardous emissions (such as NO_x, HC, PM and smoke) and thereby cause several global hazards such as acid rain, ozone depletion, greenhouse effect, climatic changes and smog [1]. On the other hand, the fuels of bio-origin have provided a tangible solution for both twin crisis i.e. fossil fuels depletion and environmental degradation [2]. Over the past three decades, several efforts have been materialized to develop alternative fuels for diesel engines based on renewable agriculture-based materials as feed stocks. In this perspective, various vegetable oils (such as Jatropha, Pongamia and Soyabean) were considered as the potential candidates to serve as a substitute fuel in diesel engines. However, the vegetable oils and their methyl esters (biodiesel) have their own limitations when they are accustomed in diesel engines. The direct usage of vegetable oils as a fuel in diesel engine is often restricted due to their high viscosity, poor atomization, incomplete combustion and carbon deposition on the fuel injectors [3,4]. Whereas, biodiesel derived from vegetable oil serves as good alternative fuel for compression ignition engines which can be mixed with diesel to reduce emissions [5,6] without affecting the engine efficiency [7]. Contrastingly, biodiesel emits exorbitant NO_x emissions owing to their high oxygen content [8].

To reduce the harmful emissions emitted from both fossil fuels and biofuels, various techniques such as exhaust gas recirculation and engine design modifications have been adopted. But those techniques that are used to reduce NO_x will lead to enhance smoke emissions, and vice versa. In order to reduce both NO_x and smoke emissions from the diesel engine, emulsification technique is widely adopted without affecting the performance characteristics of the compression ignition engine. Kass et al. [9] conducted an experiment in a four cylinder Mercedes light duty diesel engine using soybean biodiesel emulsion fuel with EGR technique and observed a high premixed combustion resulting enhanced heat release rate (as a result of prolonged ignition delay) for the biodiesel emulsion fuels compared to that of neat biodiesel operation. In addition, they have also ascertained a reduction in the NO_x and PM emissions for the biodiesel emulsion fuel compared to that of neat biodiesel operation. Kerihuel et al. [10] carried out experimental investigations in a diesel engine using methanol blended animal fat emulsion fuel (10% water, 10% of methanol, and 2% of surfactant) and observed a prolonged ignition delay due to the reduced charge temperature (on the account of water vaporization in the fuel). They also ascertained that due to the prolonged ignition delay, more fuel was accumulated in the combustion chamber for the mixture formation, and thereby enhanced the heat release rate and cylinder pressure. Dong et al. [11] studied the performance, emission and combustion characteristics of a diesel engine using ethanol–biodiesel–water micro-emulsions, and observed a high premixed combustion due to the prolonged ignition delay for the emulsion fuels compared to that of neat biodiesel operation.

Apart from some potential advantages of emulsion fuels, there are some critical problems associated with them. The prolonged ignition delay problem associated with the emulsion fuels often leads to rough engine operation, high premixed combustion rate, high heat release rate and cold-start problems [12–15]. Many researchers [15–17] have reported the problem of prolonged ignition delay with the emulsion fuel was due to the reduction in the cetane number on the addition of water.

To overcome those problems associated with the emulsion fuels, some potential additives have been adopted to eradicate the aforementioned problems. Recently, nano-additives are considered as a propitious fuel-borne catalyst to improve the fuel properties, owing to their enhanced surface area/volume ratio, quick evaporation and shorter ignition delay characteristics [18]. Very few works have been reported on incorporating the potential nanoparticles with the emulsion fuels to improve the performance, and to reduce the harmful emissions from the diesel engine.

Yetter et al. [19] and Dreizin [20] have critically reviewed the reports on the metal nanoparticle combustion and observed that the nanosize metallic powders possess high specific surface area and could lead to high reactivity. They have also revealed that adding nano-additives to the hydrocarbon fuels (such as diesel) will facilitate shortened ignition delay and reduce soot emissions. Sabourin et al. [21], Roos et al. [22] and Roger [23] have reported that adding nanosize particles to the fuel will act as a liquid fuel catalyst, and thereby enhances the ignition and combustion characteristics of the engine. Arianna et al. [24] have utilized ceria nanoparticles as a combustion improver in water/diesel emulsion fuel, and found that there was a significant reduction in the emissions such as PM, CO, HC and TEQ (Toxicity Equivalents) in a light duty vehicle diesel engine. Moy et al. [25] reported that the CNT could act as a potential nano-additive for the fuels to 1. To enhance the burning rate of the fuel; 2. To improve the cetane number; 3. To act as an anti-knock additive; 4. To promote clean burning and to suppress the smoke formation. Recently, Sadhik Basha and Anand [26–29] have conducted a series of experiments in a single cylinder diesel engine using CNT and Alumina nanoparticles as additive with diesel, biodiesel, water–diesel emulsion fuels, and observed an appreciable increase in the brake thermal efficiency and reduced harmful pollutants compared to that of neat diesel and neat biodiesel. Owing to the potential properties of CNT, the present work is aimed to establish the effects on the performance, emission and the combustion characteristics of a single cylinder direct injection diesel engine using CNT as an additive with the JME emulsion fuel.

2. Experimental setup and procedure

Engine tests were performed on a single cylinder four stroke air-cooled compression ignition engine utilized by Sadhik Basha and Anand [29]. Table 1 lists the engine specifications and operating conditions used in this study. Fig. 1 illustrates the engine, AC alternator, fuel supply lines, emission analyzers and instrumentation. The cylinder pressure was measured using a Kistler 6613CA piezoelectric pressure transducer with corresponding charge amplifier and data acquisition systems. The pressure data were taken for every 0.1 crank angle degree and the reported data were the ensemble average of 50 consecutive engine cycles. Exhaust gaseous emissions were measured by calibrated AVL DiGAS 444 analyzer, a Chemiluminescent Detector (CLD) for NO_x, a Flame Ionization Detector (FID) analyzer for HC, a Non-Dispersive Infrared (NDIR) analyzer for CO, CO_2, and a calibrated k-type chrome-alumel thermocouple to measure the exhaust gas temperature. Smoke opacity is measured by a part-flow smoke opacity meter (AVL Dismoke 437).

Table 1 Engine specifications [29].

Make/model	Kirloskar/TAF1
Type	Single cylinder, four stroke, naturally aspirated, air cooled, constant speed, direct injection
Bore × stroke	87.5 × 110 mm
Compression ratio	17.5:1
Swept volume	661 cc
Combustion chamber	Open Hemispherical
Nozzle holes	3
Spray hole diameter	0.25 mm
Spray cone angle	110°
Rated output	4.4 kW
Rated speed	1500 rpm
Injection timing	26° bTDC (static)
Injection pressure	215 bar

The engine was started with neat JME fuel and warmed up. The warm up period ended when the cooling water temperature was stabilized. Then the fuel consumption, cylinder pressure, and exhaust emissions (such as NO_x, HC, CO) and smoke opacity were measured. A similar procedure was repeated for all the tested fuels. To insure that the accuracy of the measured values, the gas analyzer was calibrated before each measurement using reference gases. All the experiments were carried out at constant speed of 1500 rpm by varying the loads at a constant injection timing of 26° bTDC (static). Tests on each fuel were repeated thrice and the averages of the measurements were noted at steady state and identical conditions, and the repeatability of all the results were found to be within 2%. ASTM standards were adopted for testing the fuel properties (Table 2). The kinematic viscosity of the fuel blends was measured at 40 °C using a Setavis Kinematic viscometer as per the ASTM D445 standards. A KEM digital density meter using the ASTM D1298 standard was employed to determine the density of the fuel blends, and the Seta Flash point testers (ASTM D93) were used to determine the flash points of the tested fuels. The calorific values of the tested fuels were determined as per the ASTM D240 standards and the ASTM test method D613 was used for the determination of cetane number of the fuel blends.

2.1. Error analysis

Table 3 sums up the measurement technique, calibrated range, accuracy and uncertainty of various instruments used in the experiment for various parameters. Errors in experiments can rise from instrument conditions, calibration, environment, observation, reading and test planning. The accuracy of the experiments has to be validated with an aid of error analysis using the method described by Moffat [30]. The analysis was performed using the differential method of propagating errors based on Taylor's theorem and the maximum error "E" of a function $f(x_1, x_2, \ldots, x_n)$ as follows:

$$E[f(x_1, x_2, \ldots, x_n)] = \sqrt{\Sigma[c_i \cdot E(x_i)]^2} \tag{2.1}$$

The percentage uncertainties of various physical quantities (such as brake thermal efficiency, brake power, specific fuel

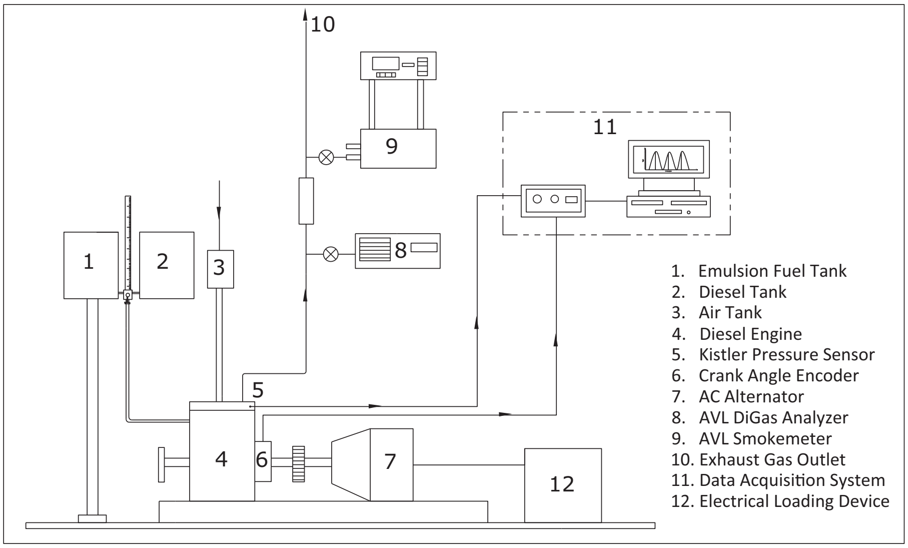

Figure 1 Schematic representation of experimental setup [29].

Table 2 Fuel properties.

Properties	JME	JME2S5W	JME2S5W25CNT	JME2S5W50CNT	JME2S5W100CNT
Density @15 °C, kg/m^3	895	899.8	897.2	897.8	899.4
Kinematic viscosity @40 °C, ($\times10^{-6}$ m^2/s)	5.05	5. 40	5.43	5.76	5.91
Flash point, °C	85	140	130	125	122
Net calorific value, MJ/kg	38.88	37.05	37.28	37.35	37.85
Cetane no.	53	51	54	55	56

Table 3 Estimated uncertainty for the measured quantities [27].

Quantity		Range	Accuracy	Uncertainty
AVL gas analyzer	NO_x	0–5000 ppm	± 10 ppm	± 0.2
	HC	0–20000 ppm	± 1 ppm	± 0.2
	CO	0–10 vol.%	0.01%	± 0.3
AVL smoke meter		0–100%	± 0.2%	± 0.1
Thermocouple		0–1000 °C	± 1 °C	± 0.2
Speed measuring unit		0–5000 rpm	± 10 rpm	± 0.5
Alternator		0–450 V, 0–20 A	± 1 V, ± 0.5 A	± 1, ± 0.2
In-cylinder pressure		0–110 bar	± 0.5 bar	± 0.1
Crank angle encoder		–	± 1°	± 0.2
Brake thermal efficiency		–	–	± 1.2

consumption) were calculated by using the percentage uncertainties of various instruments as below. If an estimated physical quantity 'E' depends on independent variables such as x_1, x_2, $x_{3,} \ldots, x_n$, then the error in the value of 'E' is calculated by:

$$\frac{\partial E}{E} = \left\{ \left(\frac{\partial x_1}{x_2}\right)^2 + \left(\frac{\partial x_2}{x_2}\right)^2 + \cdots + \left(\frac{\partial x_n}{x_n}\right)^2 \right\}^{\frac{1}{2}}. \tag{2.2}$$

where $(\partial x_1/x_1)$, $(\partial x_2/x_2)$, etc. are the errors in the independent variables, ∂x_1 is the accuracy of the measuring instrument, and x_1 is the minimum value of the output measured. The overall uncertainties were calculated using the percentage uncertainties of various instruments. The uncertainty of brake thermal efficiency (U_{bte}), pressure transducer (U_{pressure}), crank angle encoder (U_{crank}), NO_x (U_{NOx}), HC (U_{HC}) and smoke opacity (U_{smoke}) were considered to determine the overall uncertainty of the experiment. The overall uncertainty is calculated by:

$$= \sqrt{(U_{\mathrm{bte}})^2 + (U_{\mathrm{pressure}})^2 + (U_{\mathrm{crank}})^2 + (U_{NO_x})^2 + (U_{\mathrm{HC}})^2 + (U_{\mathrm{smoke}})^2}$$

$$\sqrt{(1.2)^2 + (0.1)^2 + (0.2)^2 + (0.2)^2 + (0.2)^2 + (0.1)^2}$$

$$= \pm 1.26.$$

2.2. Preparation of Jatropha Methyl Esters and JME emulsion fuel

Alkaline transesterification method was used to prepare the JME fuel process in the laboratory. The experimental procedure reported by Panwar et al. [31] was adopted for the preparation of vegetable methyl esters of Jatropha oil (Jatropha Biodiesel). The prepared JME was subjected for the preparation of JME emulsion fuel (JME2S5W).

The schematic representation of the preparation of JME emulsion fuel (JME2S5W) is depicted in Fig. 2. Initially, the importance of the surfactant was investigated for the preparation of the JME emulsion fuel. A mechanical agitator set at an agitation speed of 2000 rpm was used to mix the water and JME without surfactants for 30 min. Subsequently, the prepared fuel was kept in the test tubes for the stability investigation under static conditions. It was observed that within ten minutes there was a drastic separation of water and JME in the test tube. Henceforth, it was inferred that a bridging medium (i.e. surfactant) was needed to prepare the stable Jatropha Methyl Ester emulsion fuel. The details of surfactants with a mixture of Span80 and Tween80 and their proportions are tabulated in the Tables 4 and 5. A metering pump, reactor vessel and mechanical agitator are utilized to prepare the stable JME emulsion fuel in two phases. In the first phase, the surfactants Span80 (HLB = 4.3) and Tween80 (HLB = 15) are filled in the reactor vessel with 2% volume and subjected for agitation at a constant speed of 1000 rpm. After the agitation, both the surfactants mixed thoroughly and kept in a separate container. The magnitude of Hydrophilic–Lipophilic Balance (HLB) between the two surfactants indicates the relative strength of the hydrophilic and lipophilic

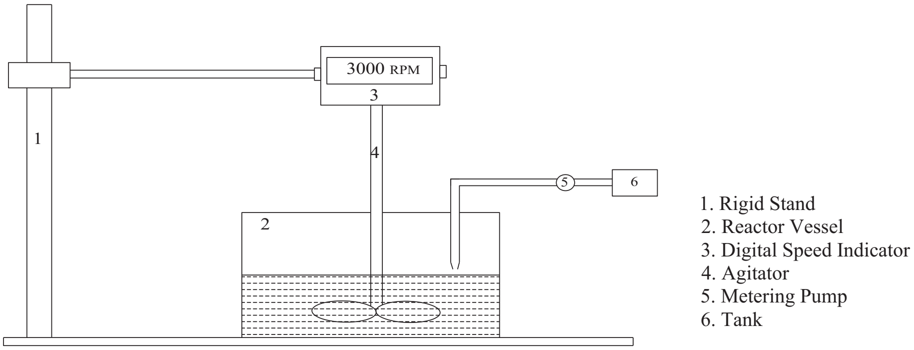

Figure 2 Schematic layout of JME emulsion fuel production set up.

Table 4 Details of Tween80 and Span80 surfactants.

Type	HLB	Specific gravity	Chemical structure
Tween80 (polyoxy ethylene sorbitan monooleate)	15	1.08	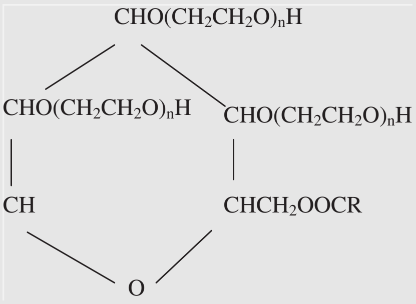
Span80 (sorbitan monooleate)	4.3	0.98	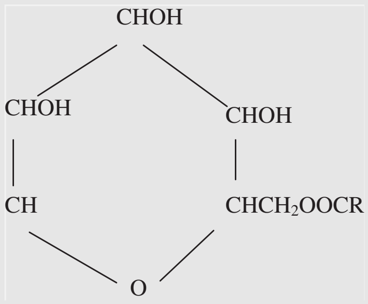

Table 5 Details of JME emulsion fuels.

Sl. no.	Emulsion fuel	Amount of CNT (ppm)	Water (%) by vol.	Biodiesel (%) by vol.	Surfactants		Stability (days)
					Span80 (%) by vol.	Tween80 (%) by vol.	
1	JME2S5W	–	5	93	1	1	5
2	JME2S5W25CNT	25	5	93	1	1	5
3	JME2S5W50CNT	50	5	93	1	1	5
4	JME2S5W100CNT	100	5	93	1	1	5

and the emulsion stability. The combined HLB value for the two surfactants is estimated using the equation [12]:

$$\mathrm{HLB}_{\mathrm{AB}} = [(H_{\mathrm{A}} * W_{\mathrm{A}}) + (H_{\mathrm{B}} * W_{\mathrm{B}})]/(W_{\mathrm{A}} + W_{\mathrm{B}}) \qquad (2.3)$$

where H_{A}, H_{B}, W_{A} and W_{B} denote the HLB values and weights of the two surfactants, Span80 and Tween80 respectively. It was found that the HLB value of 10 produced stable JME emulsion fuel and henceforth all the tested fuels were prepared of the same value. In the second phase, JME (93% by volume) was filled in the reactor vessel and it is mixed at various agitation speeds (1000–3000 rpm) with the surfactant mixture which was prepared in the first phase. In the same time, distilled water (5% by volume) was dropped by means of a metering pump at a rate of 20 mL/min in the reactor vessel. Thus, the resulting solution obtained from the reactor vessel is the JME emulsion fuel (JME2S5W) and had a creamy dark yellow color (Fig. 3). Subsequently, the JME emulsion fuels subjected for the stability investigations [32]. The following equation was adopted to find out the percentage of the separated water layer (by volume) with respect to the elapsed time [12]:

$$\text{Separated water layer }(\%) = [(\mathrm{H_2O})_{\mathrm{initial}} - (\mathrm{H_2O})_{\mathrm{final}}] * 100/(\mathrm{H_2O})_{\mathrm{initial}} \qquad (2.4)$$

where $(\mathrm{H_2O})_{\mathrm{initial}}$ denotes the initial water content, and $(\mathrm{H_2O})_{\mathrm{final}}$ denotes the final water content. It was observed that at high agitating speed (say 3000 rpm), the emulsion stability for the emulsion fuels was enhanced [12] compared to that of low agitating speeds (1500–2500 rpm) and it is graphically shown in Fig. 4. Further, it is observed that the JME2S5W fuel produced at an agitation speed of 3000 rpm was stable for

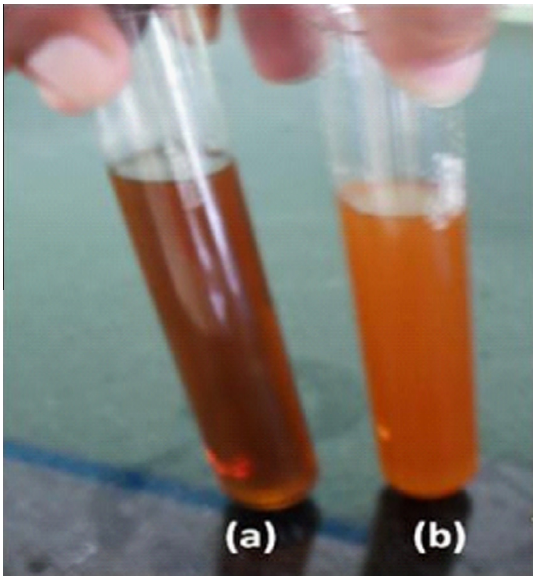

Figure 3 Photograph of (a) Jatropha Methyl Ester and (b) JME emulsion fuel.

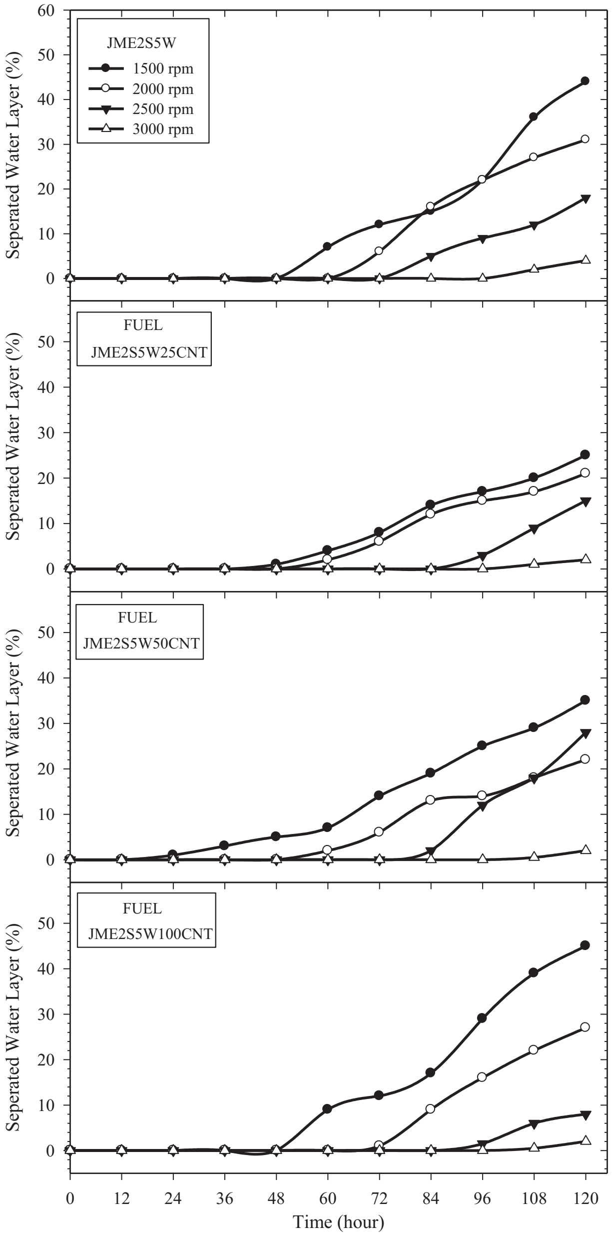

Figure 4 Stability characteristics of JME emulsion fuels.

more than five days compared to low agitating speeds (1500–2500 rpm) under static conditions.

Table 6 Details of Carbon Nanotubes.

Item	Specification
Manufacturer	NIT-Trichy, INDIA
Chemical name	CNT
Average particle size diameter (d_e)	16 nm
No. of shells (n)	2
Specific surface area	672 m^2/g
Appearance	Black

2.3. Preparation of CNT blended JME emulsion fuels

The Carbon Nanotubes were prepared by electric arc discharge method in the Institute laboratory, and its characteristics studies are reported by Sadhik Basha and Anand [26]. The detailed specifications of CNT are listed in Table 6.

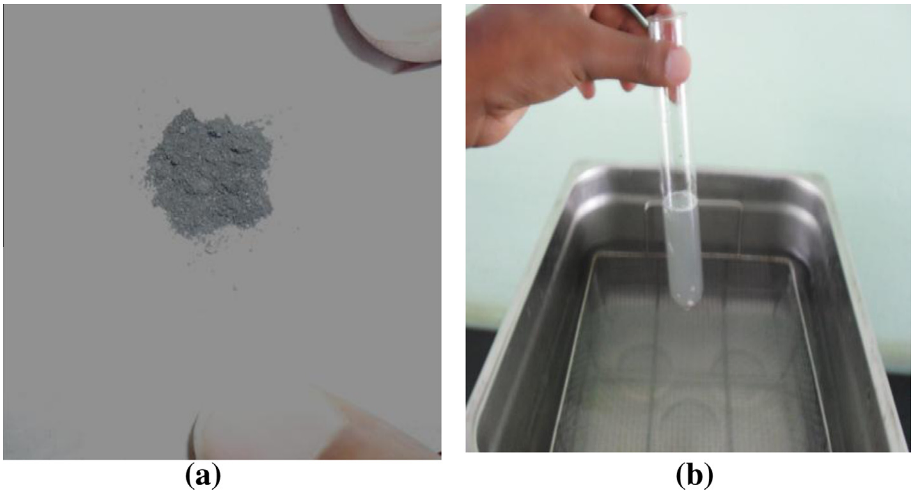

Figure 5 Photograph of (a) CNT and (b) CNT dispersed in distilled water after ultrasonication.

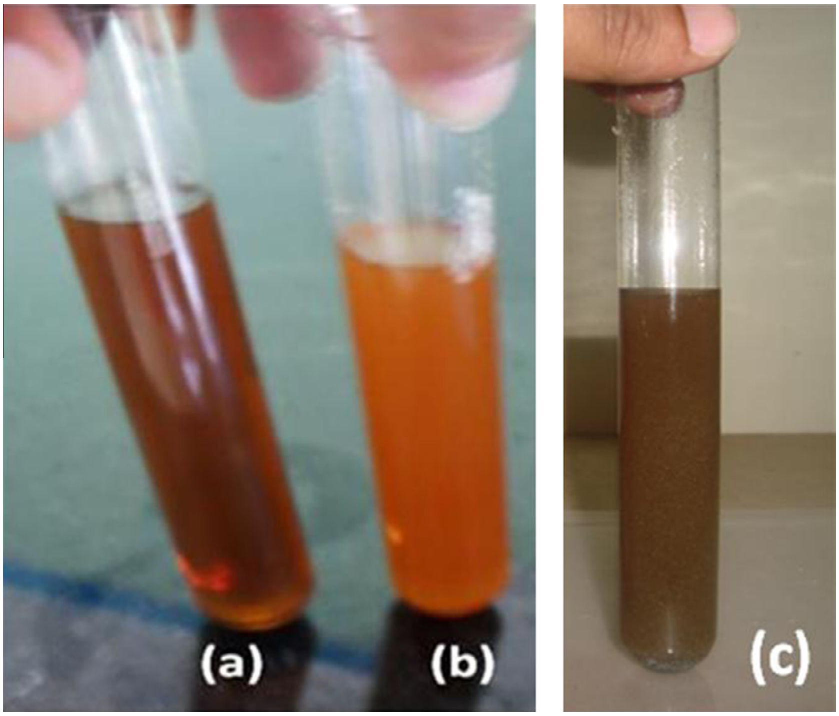

Figure 6 Photograph of (a) JME, (b) JME emulsion fuel and (c) CNT blended JME emulsion fuel.

The CNT blended JME emulsion fuels were prepared in three stages with the aid of a mechanical agitator, ultrasonicator and a reactor vessel. In the first stage, the CNTs were weighed separately by means of a digital weighing machine (Model: Shimadzu AY220, Japan) to a predefined dosage of say 25 ppm and dispersed in the distilled water (5% by volume) for 30 min with the help of an ultrasonicator and it is shown in Fig. 5. In the second stage, the surfactant mixture (Span80 and Tween80) was prepared as explained in Section 2.2. In the third stage, JME (93% by volume) was filled in the reactor vessel and it is mixed with the surfactant mixture at various agitation speeds (1000–3000 rpm). In the same time, CNT dispersed in distilled water (5% by volume) was dropped by means of a metering pump at a rate of 20 mL/min in the reactor vessel. Thus, the resulting solution obtained from the reactor vessel is the JME emulsion fuel (JME2S5W25CNT) and had a creamy dark green color (Fig. 6) and the same method was carried out for the other dosages (50 and 100 ppm) to prepare JME2S5W50CNT and JME2S5W100CNT fuels. The prepared CNT blended JME emulsion fuels at the various agitation speeds are kept in the graduated glass test tubes for the stability investigations [32]. The percentage of the separated water layer (by volume) with respect to the elapsed time was measured for each sample using Eq. (2.4). It is observed from Fig. 4 that the CNT blended JME emulsion fuels produced at an agitation speed of 3000 rpm were stable for more than five days under idle conditions. The relative volume of CNT blended JME emulsions prepared at low agitation speed (say 1500, 2000, 2500 rpm) decreased sharply with time, and hence produced unstable emulsion fuel.

3. Results and discussion

The performance, combustion and the emission characteristics of the diesel engine using neat JME, JME emulsion fuel (JME2S5W) and CNT blended JME emulsion fuels (JME2S5W25CNT, JME2S5W50CNT and JME2S5W100CNT) are investigated. Based on the combustion data, cylinder pressure and heat release rate are plotted against crank angle, whereas the ignition delay is plotted against brake mean effective pressure (bmep). The performance attributes such as brake thermal efficiency, brake specific fuel consumption, exhaust gas temperature, and the emission characteristics such as NO_x, HC and smoke opacity are plotted against bmep.

3.1. Combustion characteristics

The variation in cylinder gas pressure and the heat release rate with respect to crank angle for the JME, JME2S5W, JME2S5W25CNT, JME2S5W50CNT and JME2S5W100CNT fuels at the full load are shown in Fig. 7. The addition of CNT to the JME emulsion fuel (25, 50 and 100 ppm) has exhibited a gradual decrement in the cylinder pressure on the account of shortened premixed burning phase. This was due to the enhancement in the cetane number (Table 2) and better combustion characteristics of CNT [26]. On the other hand, the poor fuel spray pattern associated with the JME2S5W fuel could have influenced the prolonged ignition delay, thereby causing an enhancement in the premixed burning phase. As the consequence, the mean water droplet encapsulated in the JME could have delayed the auto-ignition, thereby influencing poor atomization and high dilution in the pre-flame region for the JME2S5W fuel when compared to that of CNT blended JME emulsion fuels. At the full load, the peak in-cylinder pressure for the JME fuel observed was 72.3 bar, whereas it was 79.77, 76.21, 74.11 and 72.15 bar for the JME2S5W, JME2S5W25CNT, JME2S5W50CNT and JME2S5W100CNT fuels respectively. Similar trend of enhanced heat release rate for the JME2S5W fuel was observed when compared to that of JME2S5W25CNT, JME2S5W50CNT and JME2S5W100CNT fuels. At the full load, the peak heat release rate for the JME fuel observed was 40.11 J/deg.CA, whereas it was 46.48, 42.44, 41.41 and 40.18 J/deg.CA for the JME2S5W, JME2S5W25CNT, JME2S5W50CNT and JME2S5W100CNT fuels respectively.

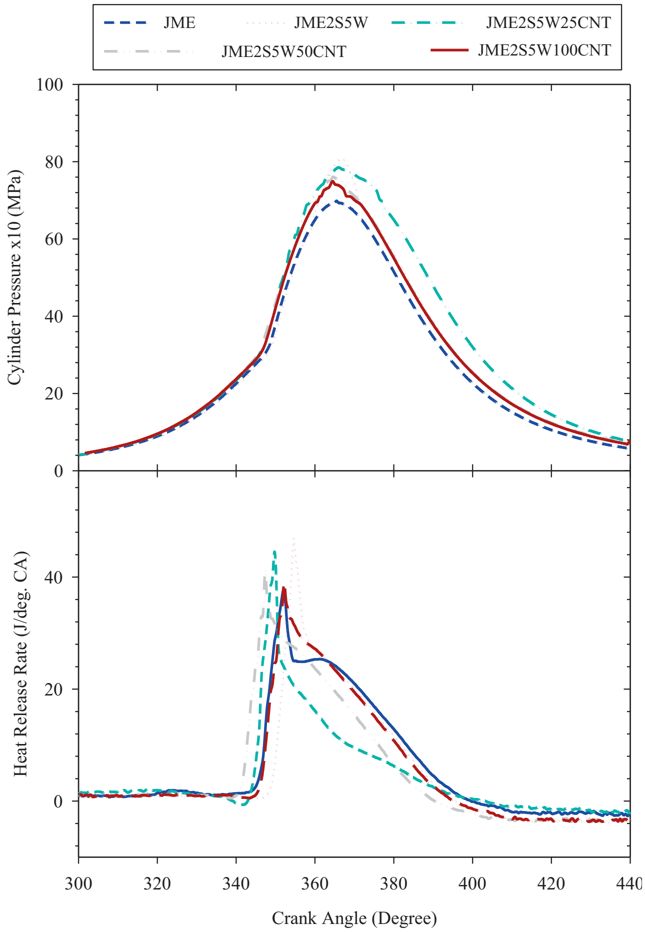

Figure 7 Variation in cylinder pressure and heat release rate with crank angle at full load.

Fig. 8 illustrates the comparison of ignition delay for the JME, JME2S5W, JME2S5W25CNT, JME2S5W50CNT and JME2S5W100CNT fuels with respect to bmep. Owing to the low calorific value (Table 2), inferior chemical reactivity [33] and significant heat absorption due to the water vaporization in the fuel jet [15,34], the magnitude of the JME2S5W fuel was prolonged compared to that of CNT blended JME emulsion fuels. Further, the dispersed water droplets in the evaporating spray have much lower boiling temperatures than the surrounding fuel. Under these conditions, they become superheated, and subsequently expand in a rapid vaporization event called micro-explosion, and in turn resulted high peak pressure. On the other hand, the addition of CNT (25, 50 and

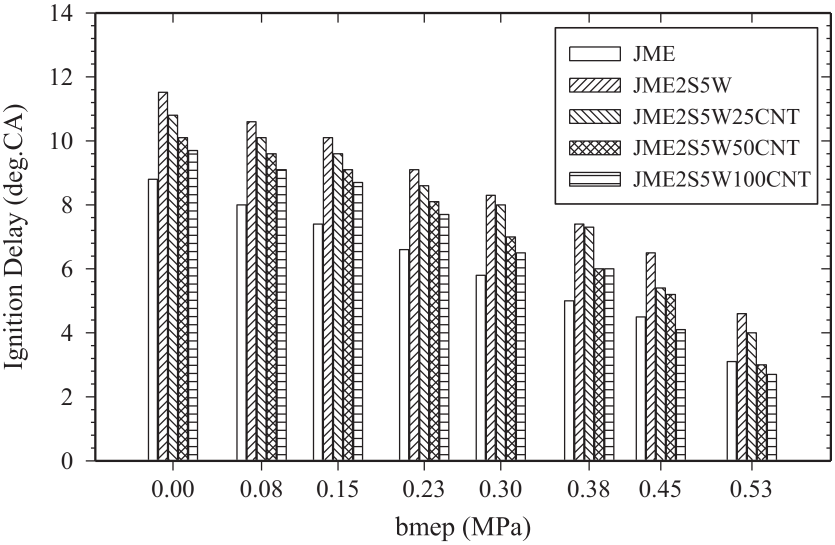

Figure 8 Variation in ignition delay for the tested fuels.

100 ppm) with the JME2S5W fuel has induced shortened premixed combustion phase (on the account of shortened ignition delay) at all the loads. The reduced ignition delay effect associated with the CNT blended JME emulsion fuels could be attributed to the enhancement in the cetane number (Refer Table 2) when compared to that of JME2S5W fuel. At the no-load and full load conditions, the ignition delay for the JME2S5W fuel was 11.52 and 4.6, whereas it was 10.8 and 4, 10.1 and 3.6 and 9.7 and 2.7 deg.CA for the JME2S5W25CNT, JME2S5W50CNT and JME2S5W100CNT fuels respectively.

3.2. Performance characteristics

The experimentally observed data are used for the evaluation of performance characteristics such as the brake thermal efficiency, brake specific fuel consumption and exhaust gas temperature and the emission characteristics such as NO_x, HC and the smoke opacity for the neat JME, JME emulsion fuel and the CNT blended JME emulsion fuels are discussed with reference to bmep.

3.3. Variation in brake thermal efficiency and brake specific fuel consumption

The variation in brake thermal efficiency for the JME, JME2S5W, JME2S5W25CNT, JME2S5W50CNT and JME2S5W100CNT fuels is shown in Fig. 9. It is observed that the brake thermal efficiency of the emulsion fuels was higher than the JME fuel due to the high heat release rate at all the loads. As the emulsion fuel gets ignited, the amount of heat release was enhanced, and caused higher brake thermal

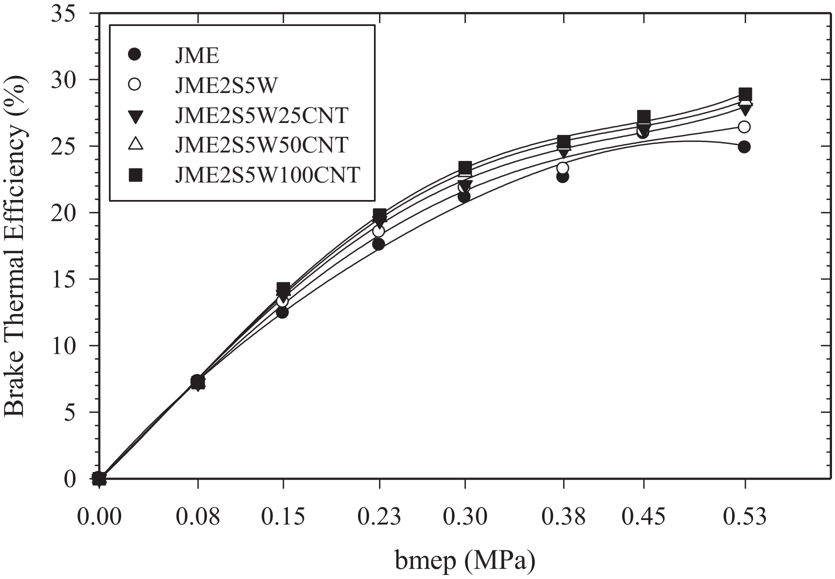

Figure 9 Variation in brake thermal efficiency for the tested fuels.

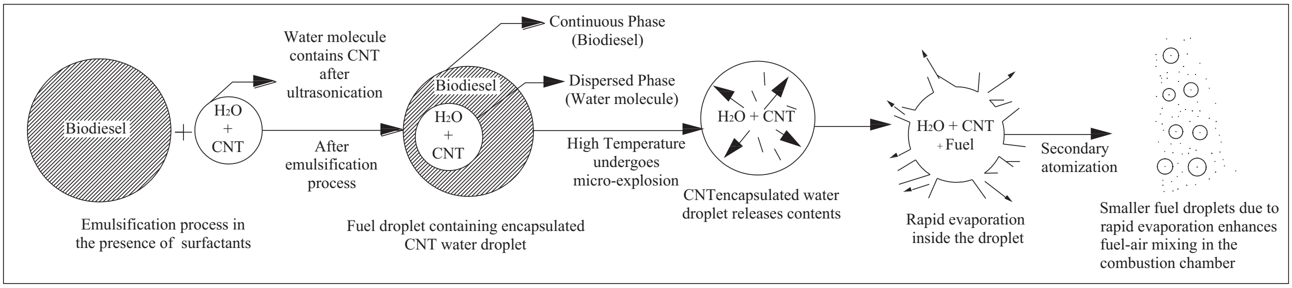

Figure 10 Micro-explosion phenomenon of CNT blended JME emulsion fuels [28].

efficiency [35] when compared to that of JME fuel. Furthermore, due to the combined effects of micro-explosion, and secondary atomization phenomenon, the combustion rate was improved [36] for the emulsion fuels when compared to that of neat JME fuel operation. On the other hand, the CNT blended JME emulsion fuels have shown further improvement in the brake thermal efficiency when compared to that of JME2S5W fuel due to the accelerated combustion. Once the CNT blended JME emulsion fuels subjected to high pressure and high temperature environment in the combustion chamber, the water droplets encased in the fuel absorbed the heat quickly (due to the low boiling point of water). As an effect, the spray jet momentum of CNT blended JME emulsion fuels could have increased, inducing intensive secondary atomization as shown in Fig. 10. Owing to the above factors, there could be an occurrence of improved homogenization of fuel and air mixing in the presence of CNT causing improved combustion and burning characteristics [26] compared to that of JME2S5W fuel. As a result, the degree of fuel–air mixing in the presence of CNT could have enhanced [26] for the CNT blended JME emulsion fuels resulting higher brake thermal efficiency compared to that of JME2S5W fuel. At the full load, the brake thermal efficiency for the JME fuel observed was 24.80%, whereas it was 26.34%, 27.89%, 28.13% and 28.45% for the JME2S5W, JME2S5W25CNT, JME2S5W50CNT and JME2S5W100CNT fuels respectively.

The enhancement in the brake thermal efficiency for the CNT blended JME emulsion fuels has reflected lower brake specific fuel consumption when compared to that of JME2S5W and JME fuel as shown in Fig. 11. The JME2S5W fuel shown higher specific fuel consumption compared to that of CNT blended JME emulsion fuels. This was due to the more fuel burning in the premixed combustion phase, and suppression of thermal dissociation (on the account of low average cylinder temperature). In addition, the JME2S5W fuel could have undergone vigorous evaporation delaying auto-ignition during the combustion. This resulted excess fuel burning in the premixed combustion phase [13] for the JME2S5W fuel leading to high brake specific fuel consumption compared to that of CNT blended JME emulsion fuels. The lower brake specific fuel consumption observed was 0.346 kg/kW h for the JME2S5W fuel, whereas it was 0.315, 0.308 and 0.301 kg/kW h for the JME2S5W25CNT, JME2S5W50CNT and JME2S5W100CNT fuels at the full load respectively.

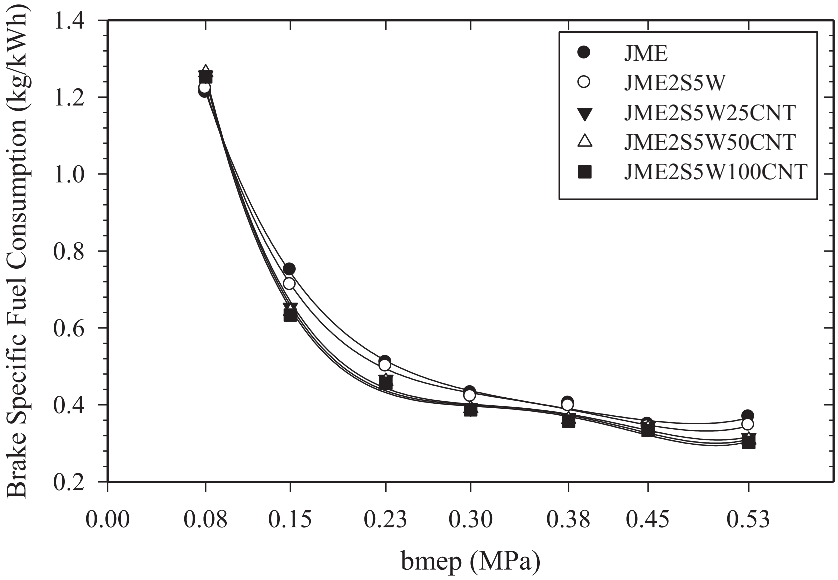

Figure 11 Variation in brake specific fuel consumption for the tested fuels.

3.4. Emission characteristics

The ensuing sections describe about the emission characteristics of the diesel engine for the tested fuels.

3.4.1. Variation of NO_x emissions

The comparison of NO_x emissions for the JME, JME2S5W, JME2S5W25CNT, JME2S5W50CNT and JME2S5W100CNT fuels is depicted in Fig. 12. The JME emulsion fuels produced lower NO_x emissions due to the significant heat sink effect during the combustion in the diesel engine. Owing to the localized lower temperature in the combustion chamber (as a result of vaporization), there could be a consequent dilution of gas species [16] associated with the JME2S5W fuel and CNT blended JME emulsion fuels leading to reduction in the NO_x emissions. On the other hand, with regard to the CNT blended JME emulsion fuels there was a further reduction of NO_x emissions when compared to that of JME and JME2S5W fuel. This could be due to improved combustion, better homogenization of reactant mixture and reduced exhaust gas temperature (Fig. 13). The encapsulated CNT water droplets in the JME emulsion fuel could have absorbed heat rapidly, thereby decreasing the burning gas temperature inside the combustion chamber, and thus could have restrained the NO_x emissions when compared to that of JME2S5W fuel. At the full load, the magnitude of NO_x emissions observed for the JME fuel was 1282 ppm, whereas it was 1001, 973, 961 and 910 ppm for the JME2S5W, JME2S5W25CNT, JME2S5W50CNT and JME2S5W100CNT fuels respectively.

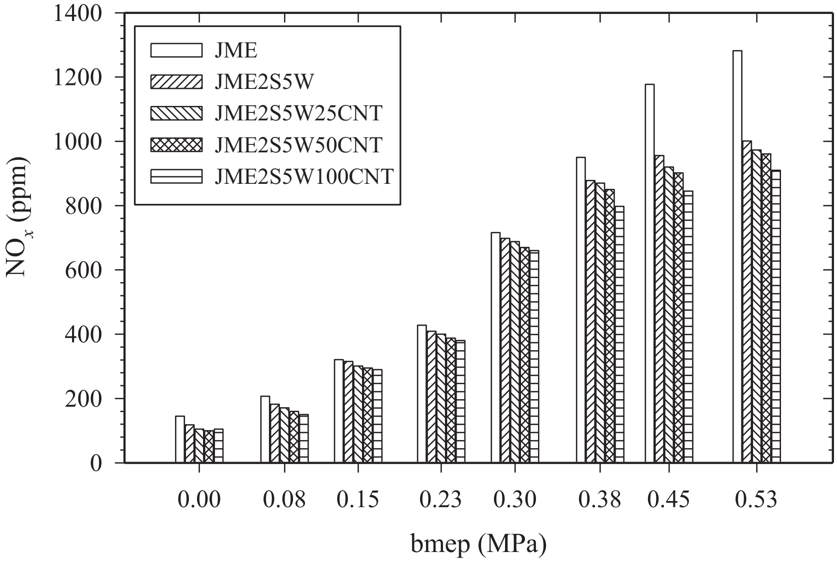

Figure 12 Variation of NO_x for the tested fuels.

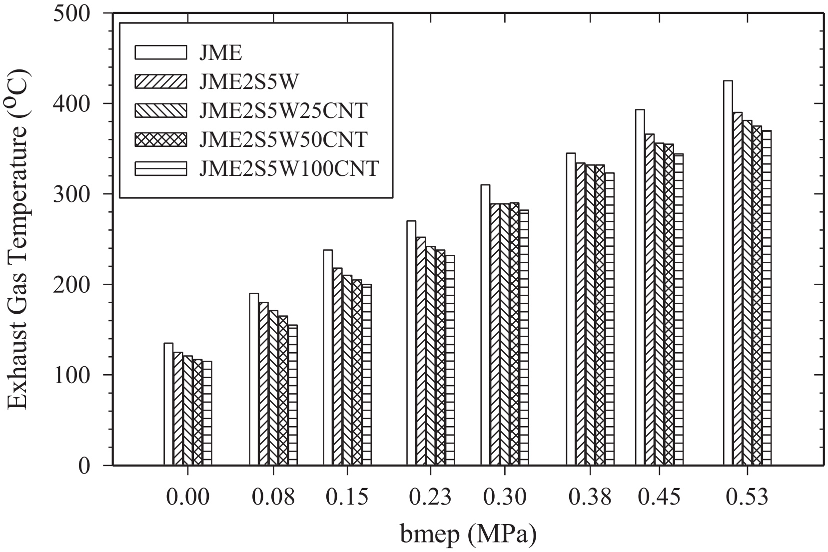

Figure 13 Variation in exhaust gas temperature for the tested fuels.

3.4.2. Variation of HC emissions

The variation of HC emission for the JME, JME2S5W, JME2S5W25CNT, JME2S5W50CNT and JME2S5W100CNT fuels is presented in Fig. 14. It was inferred from the figure that the HC emissions for the emulsion fuels were high compared to that of neat JME operation. This was due to the water content in the emulsion fuels, which have lowered the localized temperature in the combustion chamber and thereby enhanced the unburned HC emissions [37]. On the other hand, the CNT blended emulsion fuels produced a marginal reduction in the HC emissions when compared to that of JME2S5W fuel. This could be due to the intensive secondary atomization and significant fuel distribution in the presence of CNT in the combustion chamber and thereby causing the hydrocarbon oxidation. Owing to those effects, there was a marginal reduction of HC emissions for the CNT blended JME emulsion fuels when compared to that of JME2S5W fuel. At the full load, the magnitude of HC emissions observed for the JME fuel was 59 ppm, whereas it was 63, 60, 60 and 57 ppm for the JME2S5W, JME2S5W25CNT, JME2S5W50CNT and JME2S5W100CNT fuels respectively.

3.4.3. Variation of CO emissions

It is observed from Fig. 15 that the JME2S5W fuel produced higher CO emissions when compared to that of CNT blended emulsion fuels and JME. At the lower loads, the fuel supplied was less i.e., the mixture remains lean which produced lesser heat resulting in lower flame temperature, and hence there was no significant difference in the CO emissions among the tested fuels [38]. Whereas at the higher loads, the longer

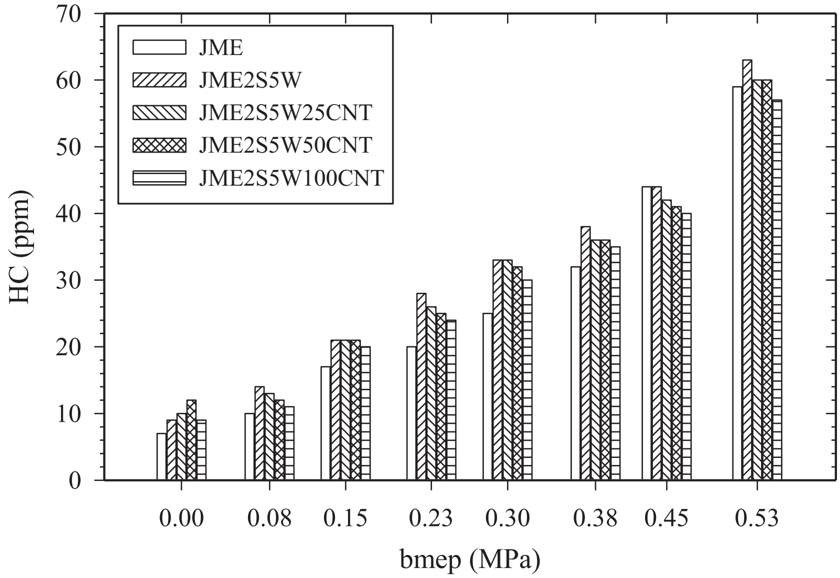

Figure 14 Variation of HC for the tested fuels.

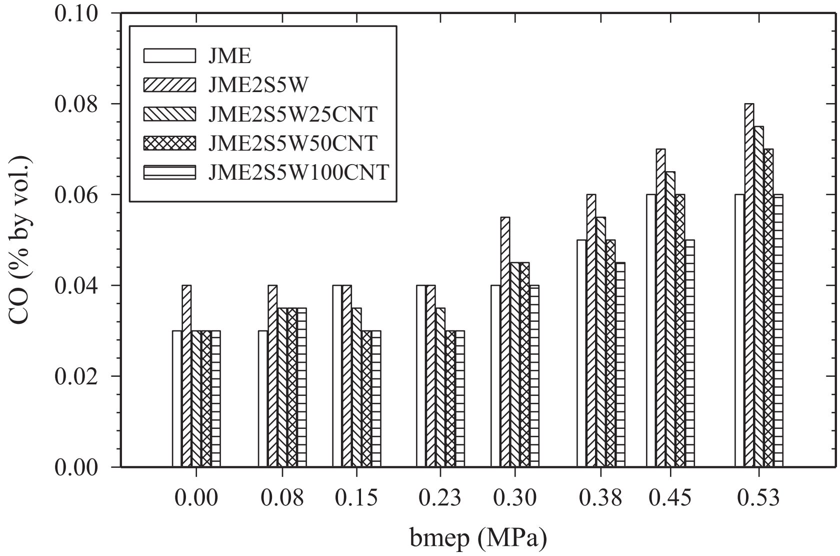

Figure 15 Variation of CO for the tested fuels.

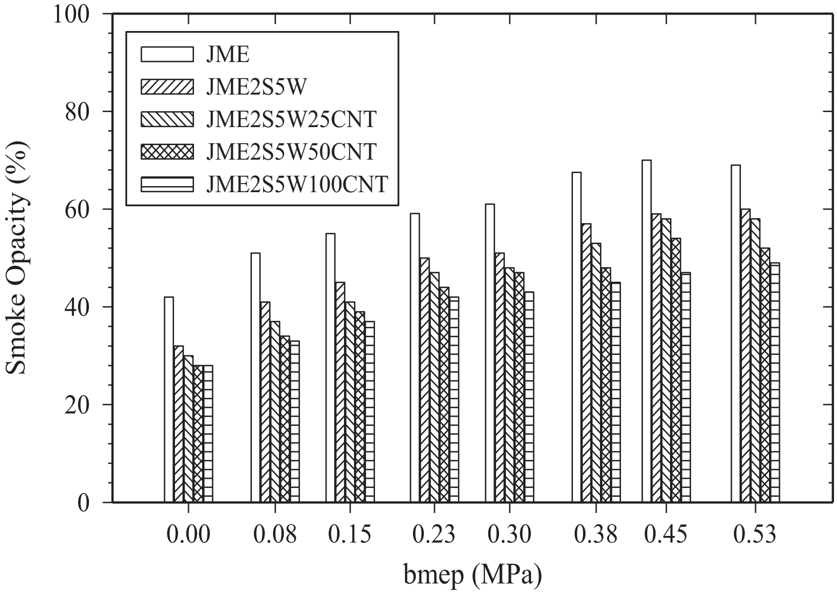

Figure 16 Variation in smoke opacity for the tested fuels.

ignition delay problem associated with the JME2S5W fuel induced poor fuel–air mixing in the engine cylinder leading to high CO emissions compared to that of JME and CNT blended emulsion fuels. On the other hand, the CNT blended emulsion fuels showed accelerated combustion due to the shortened ignition delay characteristics. Due to the shorten ignition delay effect associated with the CNT blended emulsion fuels, the degree of fuel–air mixing and uniform burning could have improved in the presence of potential CNT leading to complete combustion. Hence, there was an appreciable reduction of CO emissions for the CNT blended emulsion fuels when compared to that of JME and JME2S5W fuel. At the full load, the magnitude of CO emissions for the JME2S5W was 0.085% (by vol.), whereas it was 0.075%, 0.07% and 0.06% (by vol.) for the JME2S5W25CNT, JME2S5W50CNT and JME2S5W100CNT fuels respectively.

3.4.4. Variation in smoke opacity

The variation in smoke opacity for the JME, JME2S5W, JME2S5W25CNT, JME2S5W50CNT and JME2S5W100CNT fuels is illustrated in Fig. 16. It is observed from the figure that there is a significant reduction in the smoke emissions for the JME emulsion fuels when compared to that of neat JME. At the full load, the magnitude of the smoke opacity for the JME fuel was 69%, whereas it was 60% for the JME2S5W fuels respectively. The water content in the JME fuel has lead to significant decrement in the smoke emissions. This was due to the rapid evaporation of water vapor in the fuel-rich regions, increased spray momentum and enhancement in the OH radicals [14] which were very effective in the oxidation of soot precursors. On the other hand, the addition of CNT to the emulsion fuel has shown a pronounced effect on further reduction of smoke emissions [25,26] compared to that of JME2S5W fuel. This was likely due to the occurrence of reduced soot formation and improved reactant mixture due to the rapid secondary atomization effects [39] in the presence of CNT. At the full load, the magnitude of smoke opacity observed for the JME fuel was 69%, whereas it was 60%, 57%, 52% and 49% for the JME2S5W, JME2S5W25CNT, JME2S5W50CNT and JME2S5W100CNT fuels respectively.

4. Conclusions

The performance, emission and combustion characteristics of a direct injection diesel engine using neat JME, neat JME emulsion fuel and CNT blended JME emulsion fuels were investigated. In addition, the stability characteristics of the tested fuels were also studied. Based on the experimental investigations, the following conclusions are drawn:

(1) The stability of neat JME emulsion fuel and CNT blended JME emulsion fuels were more than five days under idle conditions. The mechanical agitation speed of 3000 rpm was found to be optimum to prepare the stable JME emulsion fuels and CNT blended JME emulsion fuels.
(2) The brake thermal efficiency of CNT blended JME emulsion fuels was appreciably enhanced owing to their improved combustion characteristics when compared to that of neat JME and neat JME emulsion fuel. At the full load, the brake thermal efficiency for the JME fuel observed was 24.80%, whereas it was 26.34% and 28.45% for the JME2S5W and JME2S5W100CNT fuels respectively.
(3) There was a significant reduction in the peak cylinder pressure and heat release rate for CNT blended JME emulsion fuels when compared to that of neat JME emulsion fuel due to the shortened ignition delay effect. At the full load, the cylinder gas pressure for the JME fuel observed was 72.3 bar, whereas it was 79.77, 76.21, 74.11 and 72.15 bar for the JME2S5W, JME2S5W25CNT, JME2S5W50CNT and JME2S5W100CNT fuels respectively.
(4) Owing to the combined effects of micro-explosion and secondary atomization associated with the CNT blended JME emulsion fuels, the level of harmful pollutants in

the exhaust gases (such as NO_x and smoke) was drastically reduced when compared to that of neat JME. At the full load, the magnitude of NO_x and smoke opacity for the neat JME was 1282 ppm and 69%, whereas it was 910 ppm and 49% for the JME2S5W100CNT fuel respectively.

Overall, it has been observed that the CNT blended emulsions has potential advantages on improving the performance and reducing the emissions from the diesel engine. However, critical investigations are also in progress to trap the possible unburnt CNT from the exhaust [40] of the diesel engine in order to safeguard the global environment.

References

[1] A. Bulent Koc, Mudhafar Abdullah, Performance and NO_x emissions of a diesel engine fueled with biodiesel–diesel–water nanoemulsions, Fuel Process. Technol. 109 (2013) 70–77.

[2] Mohammed EL-Kasaby, Medhat A. Nemit-allah, Experimental investigations of ignition delay period and performance of a diesel engine operated with Jatropha oil biodiesel, Alexandria Eng. J. 52 (2013) 141–149.

[3] Cherng-Yuan Lin, Hsiu-An Lin, Engine performance and emission characteristics of a three-phase emulsion of biodiesel produced by peroxidation, Fuel Process. Technol. 88 (2007) 35–41.

[4] S. Kent Hoekman, Curtis Robbins, Review of the effects of biodiesel on NO_x emissions, Fuel Process. Technol. 96 (2012) 237–249.

[5] S. Kalligeros, F. Zannikos, S. Stournas, E. Lois, G. Anastopoulos, Ch. Teas, et al, An investigation of using biodiesel/marine diesel blends on the performance of a stationary diesel engine, Biomass Bioenergy 24 (2003) 141–149.

[6] R. Alcantara, J. Amores, L. Canoira, E. Fidalgo, M.J. Franco, A. Navarro, Catalytic production of biodiesel from soy-bean oil, used frying oil and tallow, Biomass Bioenergy 18 (2000) 515–527.

[7] J.M. Lujan, V. Bermu dez, B. Tormos, B. Pla, Comparative analysis of a DI diesel engine fuelled with biodiesel blends during the European MVEG-A cycle: performance and emissions (II), Biomass Bioenergy 33 (2009) 948–956.

[8] Cherng-Yuan Lin, Hsiu-An Lin, Effects of NO_x-inhibitor agent on fuel properties of three-phase biodiesel emulsions, Fuel Process. Technol. 89 (2008) 1237–1242.

[9] M.D. Kass, S.A. Lewis, M.M. Swartz, S.P. Huff, D.W. Lee, R.M. Wagner, J.M.E. Storey, Utilizing water emulsification to reduce NO_x and particulate emissions associated with biodiesel, Trans. ASABE 52 (2009) 5–13.

[10] A. Kerihuel, M. Senthil Kumar, J. Bellettre, M. Tazerout, Use of animal fats as CI engine fuel by making stable emulsions with water and methanol, Fuel 84 (2005) 1713–1716.

[11] H.Q. Dong, C. Hao, F.L. Chia, M.G. Li, Z.B. Yao, Experimental studies of a naturally aspirated DI diesel engine fuelled with ethanol–biodiesel–water micro-emulsions, Energy Fuels 24 (2010) 652–663.

[12] M.Y.E. Selim, M.T. Ghannam, Performance and engine roughness of a diesel engine running on stabilized water diesel emulsion, SAE 07 NAPLES-163.

[13] M. Nadeem, C. Rangkuti, K. Anuar, M.R.U. Haq, I.B. Tan, S.S. Shah, Diesel engine performance and emission evaluation using emulsified fuels stabilized by conventional and gemini surfactants, Fuel 85 (2006) 2111–2119.

[14] K.A. Subramanian, A. Ramesh, Use of diethyl ether along with water–diesel emulsion in a DI diesel Engine, SAE 2002-01-2720.

[15] O. Armas, R. Ballesteros, F.J. Martos, J.R. Agudelo, Characterization of light duty diesel engine pollutant emissions using water-emulsified fuel, Fuel 84 (2005) 1011–1018.

[16] G. JamiL, Damon Honnery, Khaled Al-Khaleefi, Performance, emissions and heat release characteristics of direct injection diesel engine operating on diesel oil emulsion, Appl. Therm. Eng. 26 (2006).

[17] Kweonha Park, Inseok Kwak, Seungrnook Oh, The effect of water emulsified fuel on a motorway-bus diesel engine, KSME Int. J. 18 (2004) 2049–2057.

[18] H. Tyagi, P.E. Phelan, Ravi Prasher, Robert Peck, Taewoo Lee, J.R. Pacheco, Paul Arentzen, Increased hot plate ignition probability for nanoparticle-laden diesel fuel, Nano Lett. 8 (2008) 1410–1416.

[19] R.A. Yetter, G.A. Risha, S.G. Son, Metal particle combustion and nanotechnology, Proc. Combust. Inst. 32 (2009) 1819–1838.

[20] E.L. Dreizin, Phase changes in metal combustion, Prog. Energy Combust. Sci. 26 (2000) 57–78.

[21] J.L. Sabourin, M.D. Daniel, R.A. Yetter, L.D. Frederick, A.A. Ilhan, Functionalized graphene sheet colloids for enhanced fuel/propellant combustion, ACS Nano 3 (2009) 3945–3954.

[22] W.J. Roos, R. Duncan, J.C. David, Diesel fuel additives containing cerium or manganese and detergents, US Patent No. US2008/0066375 A1, 2008.

[23] S. Roger, Cerium oxide nanoparticles as fuel additives, US Patent No. US2006/0254130 A1, 2006.

[24] F. Arianna, Covadonga Astorga, Giorgio Martini, Urbano Manfredi, Anne Mueller, Maria Rey, et al, Effect of water/fuel emulsions and a cerium-based combustion improver additive on HD and LD diesel exhaust emissions, Environ. Sci. Technol. 39 (2005) 6792–6799.

[25] David Moy, Chunming Niu, Howard Tennent et al., Carbon nanotubes in fuels, US Patent 2002-6419717, 2002.

[26] J. Sadhik Basha, R.B. Anand, An experimental investigation in a diesel engine using carbon nanotubes blended water–diesel emulsion fuel, Proc. IMechE, Part A: J. Power Energy 225 (2011) 279–288.

[27] J. Sadhik Basha, R.B. Anand, An experimental study in a CI engine using nanoadditive blended water–diesel emulsion fuel, J. Green Energy 8 (2011) 332–348.

[28] J. Sadhik Basha, R.B. Anand, Role of nano-additive blended biodiesel emulsion fuel on the working characteristics of a diesel engine, J. Renew. Sust. Energy 3 (2011), http://dx.doi.org/10.1063/1.3575169.

[29] J. Sadhik Basha, R.B. Anand, Effects of nanoparticle blended water–biodiesel emulsion fuel on working characteristics of a diesel engine, J. Global Warming 2 (2010) 330–346.

[30] R.J. Moffat, Describing the uncertainties in experimental results, Exp. Therm. Fluid Sci. 1 (1988) 3–17.

[31] N.L. Panwar, Y.S. Hemant, N.S. Rathore, J. Sudhakar, A.K. Kurchania, Performance evaluation of a diesel engine fueled with methyl ester of castor oil seed oil, Appl. Therm. Eng. 30 (2010) 245–249.

[32] M.Y.E. Selim, M.T. Ghannam, Combustion study of stabilized water-in-diesel fuel emulsion, Energy Sources, Part A: Recov. Util. Environ. Effects 32 (2010) 256–274.

[33] H.W. Ching, J.T. Chen, An experimental investigation of the burning characteristics of water–oil emulsions, Int. Commun. Heat Mass Transfer 23 (1996) 823–834.

[34] J.W. Park, K.Y. Huh, J.H. Lee, Reduction of NO_x, smoke and brake specific fuel consumption with optimal injection timing and emulsion ratio of water emulsified fuel, Inst. Mech. Eng. 215 (2001) 83–93.

[35] M.K. Senthil, A. Kerihuel, J. Bellettre, M. Tazerout, Effect of water and methanol fractions on the performance of a CI engine using animal fat emulsions as fuel, Proc. IMechE Part A: J. Power Energy 219 (2005) 583–592.

[36] A.A.N. Marwan, R. Hobina, S.A. Wagstaff, The use of emulsion, water induction and EGR for controlling diesel engine emissions, SAE 2001-01-1941.

[37] M.K. Senthil, J. Bellettre, M. Tazerout, Use of biofuel emulsions as fuel for diesel engines: a review, Proc. IMechE Part A: J. Power Energy 223 (2009) 729–742.

[38] V.P. Sethi, K.S. Salariya, Exhaust analysis and performance of a single cylinder diesel engine run on dual fuels, J. Inst. Eng. 85 (2004) 1–7.

[39] T. Kadota, H. Yamasaki, Recent advances in the combustion of water fuel emulsion, Prog. Energy Combust. Sci. 28 (2002) 385–404.

[40] Suk-Won Jang, Yongin-shi, Young-Chul Joung, Suwon-shi, Apparatus for trapping carbon nanotube and system and method for producing the carbon nanotube, US Patent No. 7935175 B2, 2011.